Hindawi
Journal of Control Science and Engineering
Volume 2023, Article ID 7911672, 13 pages
https://doi.org/10.1155/2023/7911672

Research Article

Event-Triggered Quantized Stabilization of Markov Jump Systems under Deception Attacks

Jingjing Yan,[1] **Shuaibing Zhao**,[1] **and Xiaoliang Feng**[2]

[1]*College of Electrical Engineering, Henan University of Technology, Zhengzhou 450052, China*
[2]*School of Electrical Engineering, Shanghai Dianji University, Shanghai 201306, China*

Correspondence should be addressed to Shuaibing Zhao; 1731336804@qq.com

Received 19 April 2023; Revised 31 July 2023; Accepted 7 August 2023; Published 23 August 2023

Academic Editor: Petko Petkov

This paper focuses on the event-triggered quantized control for Markov jump systems with deception attacks. First, we design an event-triggered scheme relying on dwell time and end instants of attacks. It can limit the number of switches within the triggered intervals and the lower bound of triggered instants. Second, the quantization rules and the increasing/decreasing rate of Lyapunov function are obtained for different cases. Next, combined with the increasing/decreasing rate, the lower bound of triggered instants, and the probability of switches occurring, the upper bound of Lyapunov function at the triggered instants is provided. On this basis, sufficient conditions ensuring the exponential convergence in the mean sense of the closed-loop system are given. Finally, atwo-tank system is provided to verify the effectiveness of the proposed stability analysis framework for Markov jump systems.

1. Introduction

In recent years, due to the powerful modeling ability of Markov process, Markov jump systems have received extensive attention in aircraft control systems and robot systems [1–3]. Before the system data are transmitted through the network, they must be quantized and coded. Therefore, the impact of quantization errors on the system performance must be considered. Moreover, the network may suffer a malicious attack initiated by an attacker, which will seriously affect the safe operation of the system [4–6]. As a common attack method, deception attacks disrupt the system's performance by tampering with the transmitted data. Especially, in a Markov jump system, the tampered mode will result in a mode mismatch between the system side and the controller side even if the system does not switch. Thus, the system's performance is seriously reduced. Considering that the event-triggered transmission scheme can effectively reduce the amount of data transmission [7, 8], this paper will design an event-triggered quantized control strategy to guarantee the stability operation of the Markov jump systems under the influence of deception attacks.

For the Markov jump systems suffered by deception attacks, some control algorithms have been proposed to guarantee the system stability. Literature [9] designs an event-triggered scheme similar to switching according to triggered errors, switching signals, and deception attack instants to ensure the mean-square exponential input-to-state practical stability of the system. By using a novel dynamic-memory event-triggered protocol, a memory-based sliding mode control for singular semi-Markov jump systems is provided in [10] to ensure the mean-square exponential stability of the system. For Markov jump neural networks subjected to cyber-attacks, which include deception attacks and denial of service attacks, a static output feedback strategy regardless of whether hybrid cyber-attacks occur is designed in reference [11] to guarantee the specified H_∞/passive performance.

As we can see, the event-triggered scheme is a useful method to deal with the effect of deception attacks. Different from the existing results, the triggered scheme proposed in this paper does not rely on the triggered error, which can effectively avoid the Zeno behavior. Meanwhile, such scheme guarantees the existence of the lower bound of

triggered instants, which is the key point to pursue the upper bound of Lyapunov function.

Quantized control for Markov jump systems also gains fruitful results. In reference [12], a quantized iterative learning control scheme is studied by quantizing the tracking error signal based on a logarithmic quantizer. A time-triggered quantized control method is adopted in [13] to ensure the system stability. Literature [14] provides a novel switching delay quantizer with filter connections. The problem of finite-time control by using logarithmic quantizer is mainly studied in [15]. For the Markov jump system with data quantization and delay, the authors in [16] designed a hybrid-triggered mechanism and control algorithm to guarantee the asymptotic stability of the system.

If data quantization and deceptive attacks occur in a Markov jump system simultaneously, the quantized state/output and the system mode may be tampered. It is crucial to ensure the healthy operation of the system under unreliable and inaccurate data transmission. In reference [17], for uncertain fuzzy Markov switched affine systems, a compensation scheme is adopted to deal with the quantized measurement output loss intermittently, and sufficient conditions are provided such that the filtering error system is mean-square exponentially stable. In reference [18], the nonstationary quantized controller design for the Markov jump singularly perturbed systems with deception attacks is studied, and sufficient criteria are established such that the closed-loop system is stochastic mean-square exponential ultimately bounded.

Different from the existing results with logarithmic quantizer, we will adopt a time-varying uniform quantizer. Due to the fact that a uniform quantizer does not always assume that the quantizer is unsaturated such as a logarithmic quantizer, we first design the time-varying quantization radius and quantization center for different cases to guarantee the unsaturation of the quantizer. Second, a Lyapunov function is designed based on the quantization radius and quantization center, and the upper bound of which is obtained by using the lower bound of the triggered instants and the probability of the switches occurring. On this basis, sufficient conditions are given to ensure the exponential convergence in the mean sense of the closed-loop system.

Summarized above, the innovations of this paper mainly include the following three aspects: (i) an event-triggered mechanism which is independent of triggered errors is designed, which effectively avoids the Zeno behavior and meanwhile guarantees the existence of the lower bound of triggered instants; (ii) quantization rules are designed for four cases, and the upper bound of Lyapunov function at the triggered instants is obtained by combining the lower bound of triggered instants and the probability of switches occurring; and (iii) some sufficient conditions are obtained to ensure exponential convergence in the mean sense of Markov jump systems under deception attacks.

The structure of this paper is as follows: Section 2 elaborates on the problem formula, which provides a detailed description of Markov jump systems, event-triggered scheme, quantization rules, deception attacks, control rules and closed-loop systems, and the main purpose of this paper. Section 3 mainly outlines the design of quantization rules for different cases. The increasing/decreasing rate of Lyapunov function is analyzed in Section 4. On this basis, the stability analysis of the system is carried out in Section 5. Simulation and conclusions are provided in Sections 6 and 7, respectively.

1.1. Notations. The sets of nonnegative integers and nonnegative real numbers are denoted by $\mathbb{N}$ and $\mathbb{R}_{\geq 0}$. Let $\mathbb{Z} = \mathbb{N} \cup \{0\}$. The signal $\mathbb{R}^n$ represents n-dimensional Euclidean space. The ∞-norm is adopted by $\|\cdot\|$ unless otherwise specified. $\lambda(\cdot)$ and $\overline{\lambda}(\cdot)$ denote the smallest and the largest eigenvalues of a symmetric matrix, respectively.

2. Problem Formulation

The system configuration studied in this paper is shown in Figure 1. The signal flow is as follows: at time $t \in \mathbb{R}_{\geq 0}$, the sensor collects and transmits the system state $x(t)$ and the system mode $r(t)$ to the event trigger. If the trigger condition is satisfied (as shown in Section 2.2), the state $x(t_k)$ and mode $r(t_k)$ are transmitted to the quantizer at the triggered instant t_k. The quantizer quantizes the state $x(t_k)$ to c_k (the specific quantization rules are provided in Section 3). Under the role of deception attacks, if the network is attack-free, c_k and $r(t_k)$ are received by the observer. Otherwise, the tempered signals $\widetilde{c}_k$ and $\sigma(t_k)$ are adopted to update the observer state. Then, the controller designs the control algorithm according to $r(t_k)/\sigma(t_k)$ and the observer state $\widehat{x}(t)$.

2.1. Markov Jump Systems. The plant shown in Figure 1 can be modeled by the following Markovian jump systems:

$$\dot{x}(t) = A_{r(t)}x(t) + B_{r(t)}u(t), \tag{1}$$

where $x(t) \in \mathbb{R}^n$ is the system state and $u(t) \in \mathbb{R}^m$ is the control input. The switch signal $r(t) \in M = \{1, \ldots, s\}$ indicates the system mode at instant t. $A_{r(t)}$ and $B_{r(t)}$ are known matrices corresponding to different subsystems. The switching signal r satisfying the Markov jump process with dwell time is described as follows: assuming that the p-th subsystem is activated at p_i, then no switching occurs for any $t \in p_i, p_i + h)$, where $h \geq 0$ is called as the dwell time. For $t \geq p_i + h$, the switching occurs according to the transition probability matrix $\Pi = [\pi_{pq}]$, in which π_{pq} denotes the probability of the system transforming from mode $p \in M$ to mode $q \in M$, i.e., $P(r(t+\Delta) = q \mid r(t) = p) = \pi_{pq}\Delta + o(\Delta)$ for $q \neq p$ and $P(r(t+\Delta) = q \mid r(t) = p) = 1 + \pi_{pp}\Delta + o(\Delta)$ for $q = p$ with $\Delta > 0, \pi_{pq} > 0, \pi_{pp} = -\sum_{q=1,q\neq p}^{s}\pi_{pq}$ and $\lim_{\Delta \longrightarrow 0} = o(\Delta)/\Delta = 0$.

Lemma 1 (see [19]). *Let $N_r(t)$ be the switching number of $r(t)$ on the interval $(0, t)$, then we have*

$$P(N_r(t) = k) \leq e^{-\overline{\pi}t}\frac{(\pi t)^k}{k!}, \forall k \geq 0, \tag{2}$$

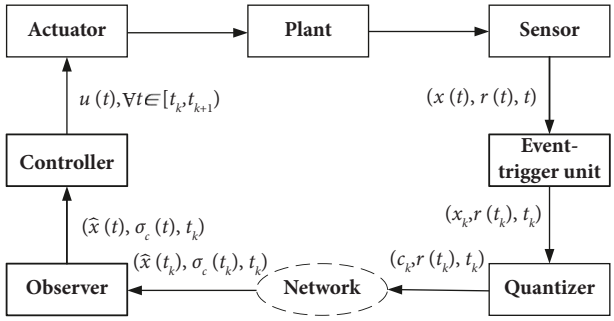

Figure 1: System configuration.

where $\overline{\pi} = \max\{\pi_{pq}: p, q \in M\}$ *and* $\pi = \max\{|\pi_{pp}|: p \in M\}$.

Assumption 2 (see [20]) (stabilizability). For each $p \in M$, the subsystem (A_p, B_p) is stabilizable, i.e., there exists a state feedback gain matrix K_p such that $A_p + B_p K_p$ is Hurwitz, i.e., all eigenvalues of $A_p + B_p K_p$ have negative real parts.

2.2. Event-Triggered Scheme. The triggered instants $\{t_k\}_{k\in\mathbb{N}}$ are determined by the following scheme:

$$t_{k+1} = \begin{cases} t_k + h, \\ t = a_m + b_m, \forall m \in \mathbb{N}, \end{cases} \tag{3}$$

where $t \geq t_k$ and $a_m + b_m$ are the end instants of deception attacks defined in Section 2.4.

The first condition is used to ensure that there is at most one switch occurring within each triggered interval. The second one ensures that transmission occurs as soon as the attack ends, which is to minimize the impact of attacks on the system's performance.

Remark 3. Although many papers have used triggered errors to design event-triggered scheme, i.e., the data are transmitted if $e_{t_k}^\top(t) N_{r(t)} e_{t_k}(t) \geq \gamma^2(t_k)$ with $e_{t_k}(t) = x(t) - x(t_k)$ [21–23], this paper does not adopt such condition for two reasons. On the one hand, if the error-based triggered condition is adopted, then the lower bound of t_k, i.e., (73) cannot be guaranteed, which makes it difficult to obtain the upper bound of the Lyapunov function. On the other hand, as shown in (23), the quantization rules designed in Section 2.3 have actually limited the range of $x(t)$, which is similar to the role of error-based triggered.

2.3. Quantization Rules. At a general triggered instant $\{t_k\}_{k\in\mathbb{N}}$, it is supposed that

$$\left\| x(t_k) - x_k^* \right\| \leq E_k, \tag{4}$$

where x_k^* is the quantization center and E_k is the half length of the quantization area. Then, we can divide the hypercube $\mathbf{S}_k := \{x \in \mathbb{R}^n: \|x - x_k^*\| \leq E_k\}$ into N^n equal hypercubic sub-boxes, N per each dimension. Let the center of the sub-box containing $x(t_k)$ be the quantized value c_k which is transmitted to the controller side along with the system mode $r(t_k)$.

Obviously, it holds the following:

$$\left\| x(t_k) - c_k \right\| \leq \frac{E_k}{N}, \tag{5}$$

and

$$\left\| c_k - x_k^* \right\| \leq \frac{N-1}{N} E_k. \tag{6}$$

Assumption 4 (see [20]) (data rate). We assume that N is large enough such that $\Lambda_p := e^{\|A_p\|h} < N, \forall p \in M$.

2.4. Deception Attacks. For any $m \in \mathbb{N}$, let $H_m = [a_m, a_m + b_m)$ with $a_m > 0$ and $b_m > 0$ indicating the m-th time interval of deception attacks. Meanwhile, $W_m = [a_m + b_m, a_{m+1})$ indicates the m-th time interval of normal communication. Obviously, for any interval $[a, b)$, $\Xi(a, b) = \bigcup_{m\in\mathbb{N}} H_m \cap (a, b)$ represents the total time interval of deception attacks on the system. Thus, in order to limit deception attacks in terms of frequency and duration, the following assumption is proposed.

Assumption 5 (see [9]). There exist $\alpha \geq 0$, $\beta \geq 0, \zeta \geq 0$, and $T \geq 1$ satisfying

$$n(a, b) \leq \alpha + \frac{b-a}{\beta}, \tag{7}$$

and

$$|\Xi(a, b)| \leq \zeta + \frac{b-a}{T}, \tag{8}$$

where $n(a, b)$ and $|\Xi(a, b)|$ represent the number and duration of deception attack in $[a, b)$, respectively. The inverses of β and T provide the upper bounds of the average number and the average duration per unit time of deception attacks, respectively. Under the effect of deception attack, the transmitted c_k and $r(t_k)$ may be tampered. To facilitate the following analysis, a binary process $\phi(t_k) \in \{0, 1\}$ is adopted to characterize the attacked situations of the network at the triggered instant t_k. Specially, $\phi(t_k) = 0$ indicates that the transmission is normal, and $\phi(t_k) = 1$ means that the network is under deception attacks.

2.5. Control Rule and Closed-Loop System. Let $\sigma_c(t_k)$ be the mode received by the controller, then the control rule is designed as follows:

$$u(t) = K_{\sigma_c(t_k)} \hat{x}(t), \forall t \in [t_k, t_{k+1}), \tag{9}$$

where $K_{\sigma_c(t_k)}$ is the feedback matrix given in Assumption 2 and $\hat{x}(t)$ is the observer state satisfying

$$\dot{\hat{x}}(t) = \left(A_{\sigma_c(t_k)} + B_{\sigma_c(t_k))} K_{\sigma_c(t_k))} \right) \hat{x}(t_k), \tag{10}$$

with

$$\hat{x}(t_k) = (1 - \phi(t_k)) c_k + \phi(t_k) \bar{c}_k. \tag{11}$$

It is assumed that the tampered quantization value $\widetilde{c}_k$ is also a center of sub-box to reduce the attack detection rate. It is obvious that if $x(t_k) \in \mathbf{S}_k$, then $\widetilde{c}_k$ meets

$$\left\|x(t_k) - \widetilde{c}_k\right\| \leq \frac{2N-1}{2N} E_k, \tag{12}$$

and

$$\left\|\widetilde{c}_k - x_k^*\right\| \leq \frac{N-1}{N} E_k. \tag{13}$$

Note that the system mode $r(t_k)$ transmitted from the system side may also be tampered. At the triggered instant t_k, we denote the tampered mode as $\sigma(t_k)$. Then,

$$\sigma_c(t_k) = (1 - \phi(t_k))r(t_k) + \phi(t_k)\sigma(t_k). \tag{14}$$

Hence, the control rule can be rewritten as

$$u(t) = \begin{cases} K_{r(t_k)} e^{\left(A_{r(t_k)} + B_{r(t_k)} K_{r(t_k)}\right)(t-t_k)} c_k, \text{if } \phi(t_k) = 0, \\ K_{\sigma(t_k)} e^{\left(A_{\sigma(t_k)} + B_{\sigma(t_k)} K_{\sigma(t_k)}\right)(t-t_k)} \widetilde{c}_k, \text{if } \phi(t_k) = 1, \end{cases} \tag{15}$$

and the closed-loop system is written as

$$\dot{x}(t) = \begin{cases} A_{r(t_k)} x(t) + B_{r(t_k)} K_{r(t_k)} \\ \times e^{\left(A_{r(t_k)} + B_{r(t_k)} K_{r(t_k)}\right)(t-t_k)} c_k, \text{if } \phi(t_k) = 0, \\ A_{r(t_k)} x(t) + B_{r(t_k)} K_{\sigma(t_k)} \\ \times e^{\left(A_{\sigma(t_k)} + B_{\sigma(t)} K_{\sigma(t_k)}\right)(t-t_k)} \widetilde{c}_k, \text{if } \phi(t_k) = 1. \end{cases} \tag{16}$$

2.6. Main Objective. Similar to the exponential convergence defined in [20], the property of exponential convergence in the mean sense is defined as follows.

Definition 6. The closed-loop system (16) is exponential convergence in the mean sense that if there exist constants $\eta > 0$ and $\omega > 0$ and a function: $(0, \infty) \longrightarrow (0, \infty)$ such that

$$E(\|x(t)\|) \leq \eta e^{-\omega t} g(\|x(0)\|), \forall t \geq 0. \tag{17}$$

The control objective of this paper is designing the suitable quantization rules and a controller with the feedback matrix defined in Assumption 2 such that the closed-loop system (16) is the exponential convergence in the mean sense.

3. The Design of Quantization Rules

From Section 2.3, we should guarantee that (4) always holds for any triggered instant $\{t_k\}_{k\in\mathbb{N}}$. To achieve this purpose, we first pursue an initial instant t_0 and an initial hypercubic box $\mathbf{S}_0 = \{x \in \mathbb{R}^n : \|x(t_0) - x_0^*\| \leq E(t_0)\}$ with $x_0^* = 0_{n*n}$ such that $x(t_0) \in \mathbf{S}_0$.

Let $u(t) = 0$, then system (1) is operated in an open-loop. For any given constants $E_0 > 0$ and $\overline{\delta} > 0$, it defines an increasing function as follows:

$$E(t) := e^{(1+\overline{\delta})\max_{p\in M}\|A_p\|t} E_0. \tag{18}$$

Due to that $E(t)$ grows fast to dominate the growth rate of the open-loop dynamics. It must be a finite time t_0 such that $\|x(t_0)\| \leq E(t_0)$, i.e., $x(t_0) \in \mathbf{S}_0$. Denote t_0 as the initial triggered instant, and turn the system (1) to the closed-loop form for any $t \geq t_0$.

Next, we will give an iterative design method for quantization rules. Assuming that (4) holds, E_{k+1} and x_{k+1}^* will be designed such that

$$\left\|x(t_{k+1}) - x_{k+1}^*\right\| \leq E_{k+1}, \tag{19}$$

is satisfied for different cases.

3.1. Triggered Interval with No Switch. To facilitate the following analysis, for any system mode $r(t) = \widetilde{p} \in M$ and the controller mode $\sigma_c(t_k) = \widetilde{q} \in M$, we define the matrix $\overline{A}_{\widetilde{q}\widetilde{p}}$ as follows:

$$\overline{A}_{\widetilde{q}\widetilde{p}} = \begin{bmatrix} A_{\widetilde{p}} & B_{\widetilde{p}} K_{\widetilde{q}} \\ 0 & A_{\widetilde{q}} + B_{\widetilde{q}} K_{\widetilde{q}} \end{bmatrix}. \tag{20}$$

3.1.1. No Attack Occurs at t_k. If $r(t_k) = r(t_{k+1}) = p \in M$ and $\phi(t_k) = 0$, the error $e := x - \widehat{x}$ satisfies $\dot{e}(t) = A_p e(t)$, $\forall t \in [t_k, t_{k+1})$. Due to $\|e(t_k)\| \leq E_k/N$ by recalling (5) and (11), one has

$$\left\|e(t_{k+1}^-)\right\| \leq \Lambda_p \frac{E_k}{N} =: E_{k+1}, \tag{21}$$

with Λ_p defined in Assumption 4. To ensure (19), we can let

$$x_{k+1}^* := \widehat{x}(t_{k+1}^-) = e^{\left(A_p + B_p K_p\right)(t_{k+1} - t_k)} c_k. \tag{22}$$

3.1.2. An Attack Occurs at t_k. For $\phi(t_k) = 1$, we denote the system mode as $r(t_k) = r(t_{k+1}) = p \in M$ and the tampered mode as $\sigma(t_k) = m \in M$. On the triggered interval $[t_k, t_{k+1})$, the close-loop dynamics are

$$\begin{bmatrix} \dot{x}(t) \\ \dot{\widehat{x}}(t) \end{bmatrix} = \begin{bmatrix} A_p & B_p K_m \\ 0 & A_m + B_m K_m \end{bmatrix} \begin{bmatrix} x(t) \\ \widehat{x}(t) \end{bmatrix}. \tag{23}$$

Let $y := \begin{bmatrix} x \\ \widehat{x} \end{bmatrix}$, (23) can be rewritten as

$$\dot{y}(t) = \overline{A}_{mp} y(t). \tag{24}$$

By (11) and (12), we can easily get

$$\left\| y(t_k) - \begin{bmatrix} \widehat{x}(t_k) \\ \widehat{x}(t_k) \end{bmatrix} \right\| \leq \left\|x(t_k) - \widehat{x}(t_k)\right\| \leq \frac{2N-1}{2N} E_k. \tag{25}$$

By introducing an auxiliary system

$$\dot{\overline{y}}(t) = \overline{A}_{mp}\overline{y}(t), \overline{y}(0) = \begin{bmatrix} \hat{x}(t_k) \\ \hat{x}(t_k) \end{bmatrix}, \tag{26}$$

we know that

$$\begin{aligned} &\left\| y(t_{k+1}) - \overline{y}(t_{k+1} - t_k) \right\| \\ &\quad \le \left\| e^{\overline{A}_{mp}(t_{k+1}-t_k)} \right\| \frac{2N-1}{2N} E_k := E_{k+1}. \end{aligned} \tag{27}$$

Moreover, x_{k+1}^* is designed by projecting $\overline{y}(t_{k+1} - t_k)$ onto the x component

$$\begin{aligned} x_{k+1}^* &:= [I_{n*n}\, 0_{n*n}]\overline{y}((t_{k+1} - t_k)) \\ &= [I_{n*n}\, 0_{n*n}] e^{\overline{A}_{mp}(t_{k+1}-t_k)} \begin{bmatrix} I_{n*n} \\ I_{n*n} \end{bmatrix} \widetilde{c}_k. \end{aligned} \tag{28}$$

3.2. Triggered Interval with a Switch

3.2.1. No Attack Occurs at t_k. Suppose that $r(t_k) = p$ and $r(t_{k+1}) = q \neq p$. Similar to the analysis in Section 4.2 of [20], E_{k+1} and x_{k+1}^* can be designed as follows:

$$\begin{aligned} E_{k+1} &= \left(e^{\left\| \overline{A}_{pq} \right\| \max\{t'', t_{k+1}-t_k-t''\}} + 1 \right) \left\| e^{\overline{A}_{pq}t''} \right\| \left\| e^{\left(A_p + B_p K_p\right)t'} \right\| \\ &\quad \times \left(\left\| x_k^* \right\| + \frac{N-1}{N} E_k \right) + e^{\left\| \overline{A}_{pq} \right\| (t_{k+1}-t_k)} \\ &\quad \times \left(\left(e^{\left\| A_p + B_p K_p \right\| \max\{t', t_{k+1}-t_k-t'\}} + 1 \right) \left\| e^{\left(A_p + B_p K_p\right)t'} \right\| \right. \\ &\quad \left. \times \left(\left\| x_k^* \right\| + \frac{N-1}{N} E_k \right) + e^{\left\| A_p \right\| (t_{k+1}-t_k)} \frac{E_k}{N} \right), \end{aligned} \tag{29}$$

and

$$x_{k+1}^* := [I_{n*n}\, 0_{n*n}] e^{\overline{A}_{pq}t''} \begin{bmatrix} I_{n*n} \\ I_{n*n} \end{bmatrix} e^{\left(A_p + B_p K_p\right)t'} c_k, \tag{30}$$

where t' and t'' are any given constants belonging to $[0, t_{k+1} - t_k]$.

3.2.2. An Attack Occurs at t_k. Let $r(t_k) = p$, $r(t_{k+1}) = q \neq p$, and $\sigma(t_k) = m$. Obviously, there is an unknown instant $t_k + \overline{t}$ such that $r(t) = p, \forall t \in [t_k, t_k + \overline{t})$ and $r(t) = q, \forall t \in [t_k + \overline{t}, t_{k+1})$.

(a) Analysis before the Switch. On $[t_k, t_k + \overline{t})$, similar to the analysis of (23)–(27), we have

$$\left\| y(t_k + \overline{t}) - \overline{y}(\overline{t}) \right\| \le \left\| e^{\overline{A}_{mp}\overline{t}} \right\| \frac{2N-1}{2N} E_k. \tag{31}$$

For any $t' \in [0, t_{k+1} - t_k]$, it is easy to see that

$$\begin{aligned} &\left\| \overline{y}(\overline{t}) - \overline{y}\left(t'\right) \right\| \\ &\quad \le \left\| e^{\overline{A}_{mp}(\overline{t}-t')} \right\| \left\| e^{\overline{A}_{mp}t'} \right\| \left\| \overline{y}(0) \right\| \\ &\quad \le \left\| e^{\overline{A}_{mp}(\overline{t}-t')} \right\| \left\| e^{\overline{A}_{mp}t'} \right\| \left\| \widetilde{c}_k \right\| \\ &\quad \le \left\| e^{\overline{A}_{mp}(\overline{t}-t')} \right\| \left\| e^{\overline{A}_{mp}t'} \right\| \left(\left\| x_k^* \right\| + \frac{N-1}{N} E_k \right). \end{aligned} \tag{32}$$

By recalling (13), the triangle inequality, it obtains

$$\begin{aligned} &\left\| y(t_k + \overline{t}) - \overline{y}\left(t'\right) \right\| \\ &\quad \le \left\| e^{\overline{A}_{mp}(\overline{t}-t')} \right\| \left\| e^{\overline{A}_{mp}t'} \right\| \left(x_k^* + \frac{N-1}{N} E_k \right) \\ &\qquad + \left\| e^{\overline{A}_{mp}\overline{t}} \right\| \frac{2N-1}{2N} E_k \\ &\quad =: D_{k+1}(\overline{t}). \end{aligned} \tag{33}$$

(b) Analysis after the Switch. On the interval $[t_k + \overline{t}, t_{k+1})$, the closed-loop dynamic is as follows:

$$\dot{y} = \overline{A}_{mq} y. \tag{34}$$

Considering the second auxiliary system as follows:

$$\dot{\widetilde{y}} = \overline{A}_{mq}\widetilde{y}, \widetilde{y}(0) = \overline{y}\left(t'\right), \tag{35}$$

one can see that

$$\left\| y(t_{k+1}^-) - \widetilde{y}(t_{k+1} - t_k - \overline{t}) \right\| \le \left\| e^{\overline{A}_{mq}(t_{k+1}-t_k-\overline{t})} \right\| D_{k+1}(\overline{t}). \tag{36}$$

To eliminate the dependence of the quantization center on the unknown time $\overline{t}$, we pick a $t'' \in [0, t_{k+1} - t_k]$. Then, it yields

$$\begin{aligned} &\left\| \widetilde{y}(t_{k+1} - t_k - \overline{t}) - \widetilde{y}\left(t''\right) \right\| \\ &\quad \le \left\| e^{\overline{A}_{mq}(t_{k+1}-t_k-\overline{t}-t'')} - I \right\| \left\| \widetilde{y}\left(t''\right) \right\| \\ &\quad \le \left\| e^{\overline{A}_{mq}(t_{k+1}-t_k-\overline{t}-t'')} - I \right\| \left\| e^{\overline{A}_{mq}t''} \right\| \left\| \widetilde{y}(0) \right\| \\ &\quad = \left\| e^{\overline{A}_{mq}(t_{k+1}-t_k-\overline{t}-t'')} - I \right\| \left\| e^{\overline{A}_{mq}t''} \right\| \left\| e^{\overline{A}_{mp}t'} \right\| \left\| \overline{y}(0) \right\| \\ &\quad \le \left\| e^{\overline{A}_{mq}(t_{k+1}-t_k-\overline{t}-t'')} - I \right\| \left\| e^{\overline{A}_{mq}t''} \right\| \left\| e^{\overline{A}_{mp}t'} \right\| \\ &\qquad \times \left(\left\| x_k^* \right\| + \frac{N-1}{N} E_k \right). \end{aligned} \tag{37}$$

Combined with the above inequalities, one has

$$\begin{aligned}
&\left\|y\left(t_{k+1}^{-}\right)-\tilde{y}\left(t^{''}\right)\right\| \\
&\leq\left\|e^{\overline{A}_{mq}\left(t_{k+1}-t_k-\bar{t}-t^{''}\right)}-I\right\|\left\|e^{\overline{A}_{mq}t^{''}}\right\|\left\|e^{\overline{A}_{mp}t^{'}}\right\| \\
&\quad\times\left(\left\|x_k^*\right\|+\frac{N-1}{N}E_k\right)+\left\|e^{\overline{A}_{mq}\left(t_{k+1}-t_k-\bar{t}\right)}\right\|D_{k+1}(\bar{t}) \\
&\leq\left(e^{\left\|\overline{A}_{mq}\right\|\left(t_{k+1}-t_k-t^{''}\right)}+1\right)\left\|e^{\overline{A}_{mq}t^{''}}\right\|\left\|e^{\overline{A}_{mp}t^{'}}\right\| \\
&\quad\times\left(\left\|x_k^*\right\|+\frac{N-1}{N}E_k\right)+e^{\left\|\overline{A}_{mq}\right\|\left(t_{k+1}-t_k\right)} \\
&\quad\times e^{\left\|\overline{A}_{mp}\right\|\left(t_{k+1}-t_k\right)}\left(\left\|x_k^*\right\|+\frac{4N-3}{2N}E_k\right):=E_{k+1},
\end{aligned}\tag{38}$$

by using the properties $\|M-I\|\leq\|M\|+1$ and $\|e^{As}\|\leq e^{\|A\|}|s|$. Moreover, x_{k+1}^* can be defined as follows:

$$\begin{aligned}
x_{k+1}^* &:= [I_{n*n}\,0_{n*n}]\tilde{y}\left(t^{''}\right) \\
&= [I_{n*n}\,0_{n*n}]e^{\overline{A}_{mq}t^{''}}e^{\overline{A}_{mp}t^{'}}\tilde{c}_k.
\end{aligned}\tag{39}$$

4. Increasing/Decreasing Rate of Lyapunov Function

Let $r(t_k)=p$ denote $\tau_k=t_{k+1}-t_k\in(0,h)$. According to Assumption 2, there exist positive-definite matrices $P_p(\tau_k)$ and $Q_p(\tau_k)$ such that $S_p(\tau_k)^TP_p(\tau_k)S_p(\tau_k)-P_p(\tau_k)=-Q_p(\tau_k)<0$, with $S_p(\tau_k)=e^{(A_p+B_pK_p)\tau_k}$. Defining

$$\beta_{1,p}:=\left(\frac{2n^2\widetilde{S}_p^2}{\overline{Q}_p}+n\widetilde{S}_p\right)\left(\frac{N-1}{N}\right)^2,\tag{40}$$

where $\widetilde{S}_p=\max_{\tau_k\in(0,h]}\|S_p(\tau_k)^TP_p(\tau_k)S_p(\tau_k)\|$ and $\overline{Q}_p=\min_{\tau_k\in(0,h]}\lambda(Q_p(\tau_k))$, there must exist a large enough positive constant ρ_p such that

$$\frac{\beta_{1,p}}{\rho_p}+\frac{\Lambda_p^2}{N^2}<1,\tag{41}$$

by recalling Assumption 5. Obviously, such defined $\beta_{1,p}$ can eliminate the dependency of ρ_p on τ_k. However, the matrix P_p that satisfies $S_p(\tau_k)^TP_p(\tau_k)S_p(\tau_k)-P_p(\tau_k)=-Q_p(\tau_k)<0$ solved by linear matrix inequality always changes with the value of τ_k. Then, we define Lyapunov function as

$$V_p(x_k^*,E_k):=(x_k^*)^\top P_p(\tau_k)x_k^*+\rho_pE_k^2.\tag{42}$$

This section will provide the increasing/decreasing rate of such Lyapunov function for different cases, which is the basis of stability analysis.

4.1. Triggered Interval with No Switch

4.1.1. No Attack Occurs at t_k. If $r(t_k)=r(t_{k+1})=p\in M$ and $\phi(t_k)=0$, one has $E_{k+1}=\Lambda_pE_k/N$ and $x_{k+1}^*=S_p(\tau_k)c_k$ by recalling (21) and (22).

Similar to the analysis in [20], one gets the following:

$$V_p(x_{k+1}^*,E_{k+1})\leq\mu_1V_p(x_k^*,E_k),\tag{43}$$

where

$$\begin{aligned}
\mu_1&=\max_{p\in M}\mu_{1p},\\
\mu_{1p}&=\max\left\{1-\frac{0.5\overline{Q}_p}{n\widetilde{P}_p},\frac{\beta_{1,p}}{\rho_p}+\left(\frac{\Lambda_p}{N}\right)^2\right\}<1,
\end{aligned}\tag{44}$$

with $\widetilde{P}_p=\max_{\tau_k\in(0,h]}\overline{\lambda}(P_p(\tau_k))$.

4.1.2. An Attack Occurs at t_k. If $\phi(t_k)=1$, let $r(t_k)=r(t_{k+1})=p\in M$ and $\sigma(t_k)=m\in M$. It follows from (28) that $x_{k+1}^*=H_{mp}(\tau_k)\tilde{c}_k$ with $H_{mp}(\tau_k)$ defined by the following:

$$H_{mp}(\tau_k):=[I_{n*n}\,0_{n*n}]e^{\overline{A}_{mp}(\tau_k)}\begin{bmatrix}I_{n*n}\\I_{n*n}\end{bmatrix}.\tag{45}$$

It gives that

$$\left\|x_{k+1}^*\right\|\leq h_{mp}\left(\left\|x_k^*\right\|+\frac{N-1}{N}E_k\right),\tag{46}$$

with $h_{mp}:=\max_{\tau_k\in(0,h]}\|H_{mp}(\tau_k)\|$. Moreover, we know from (27) that

$$E_{k+1}\leq e^{\left\|\overline{A}_{mp}\right\|h}E_k:=\beta_{2,mp}E_k.\tag{47}$$

Since $\|x\|\leq|x|\leq\sqrt{n}\|x\|$, where $|x|$ denotes the Euclidean norm of the vector x, it yields

$$\begin{aligned}
&V_p(x_{k+1}^*,E_{k+1})\\
&\quad=(x_{k+1}^*)^\top P_p(\tau_{k+1})x_{k+1}^*+\rho_pE_{k+1}^2\\
&\quad\leq n\overline{\lambda}\left(P_p(\tau_{k+1})\right)\left\|x_{k+1}^*\right\|^2+\rho_pE_{k+1}^2\\
&\quad\leq n\widetilde{P}_ph_{mp}^2\left(\left\|x_k^*\right\|+\frac{N-1}{N}E_k\right)^2+\rho_p\left(\beta_{2,mp}E_k\right)^2\\
&\quad\leq 2n\widetilde{P}_ph_{mp}^2\left\|x_k^*\right\|^2+2n\widetilde{P}_ph_{mp}^2\left(\frac{N-1}{N}\right)^2E_k^2+\rho_p\beta_{2,mp}^2E_k^2\\
&\quad=\left(2n\widetilde{P}_ph_{mp}^2\right)\left\|x_k^*\right\|^2\\
&\qquad+\left(2n\widetilde{P}_ph_{mp}^2\left(\frac{N-1}{N}\right)^2+\rho_p\beta_{2,mp}^2\right)E_k^2\\
&\quad\leq\frac{2n\widetilde{P}_ph_{mp}^2}{\underline{\lambda}\left(P_p(\tau_k)\right)}(x_k^*)^\top P_p(\tau_k)x_k^*\\
&\qquad+\left(\frac{2n\widetilde{P}_ph_{mp}^2}{\rho_p}\left(\frac{N-1}{N}\right)^2+\beta_{2,mp}^2\right)\rho_pE_k^2\\
&\quad\leq\mu_2V_p(x_k^*,E_k),
\end{aligned}\tag{48}$$

where

$$\mu_2 = \max_{p,m\in M}\mu_{2mp},$$

$$\mu_{2mp} = \max\left\{\frac{2n\widetilde{P}_p h_{mp}^2}{\overline{P}_p}, \frac{2n\widetilde{P}_p h_{mp}^2}{\rho_p}\left(\frac{N-1}{N}\right)^2 + \beta_{2,mp}^2\right\}, \tag{49}$$

with $\overline{P}_p = \min_{\tau_k\in(0,h]}\lambda(P_p(\tau_k))$.

4.2. Triggered Interval with a Switch

4.2.1. No Attack Occurs at t_k. When $r(t_k) = p, r(t_{k+1}) = q \neq p$ and $\phi(t_k) = 0$, (29) and (30) yield

$$E_{k+1} \le \alpha_{3,pq}\left\|x_k^*\right\| + \beta_{3,pq}E_k, \tag{50}$$

where

$$\begin{aligned}\alpha_{3,pq} &= \left(e^{\left\|\overline{A}_{pq}\right\|\max\{t'',h-t''\}} + 1\right)\left\|e^{\overline{A}_{pq}t''}\right\|\left\|e^{\left(A_p+B_pK_p\right)t'}\right\| \\ &\quad + e^{\left\|\overline{A}_{pq}\right\|h}\left(e^{\left\|A_p+B_pK_p\right\|\max\{t',h-t'\}} + 1\right) \\ &\quad \times\left\|e^{\left(A_p+B_pK_p\right)t'}\right\|, \\ \beta_{3,pq} &= \alpha_{3,pq}\frac{N-1}{N} + e^{\left\|\overline{A}_{pq}\right\|h}e^{\left\|A_p\right\|h}\frac{1}{N}, \\ \left\|x_{k+1}^*\right\| &\le \widetilde{h}_{pq}\left(\left\|x_k^*\right\| + \frac{N-1}{N}E_k\right),\end{aligned} \tag{51}$$

with $\widetilde{h}_{pq} = \|\widetilde{H}_{pq}\|$ and

$$\widetilde{H}_{pq} := [I_{n*n}\,0_{n*n}]e^{\overline{A}_{pq}t''}\begin{bmatrix} I_{n*n} \\ I_{n*n}\end{bmatrix}e^{\left(A_p+B_pK_p\right)t'}. \tag{52}$$

Similar to the proof of Lemma 7 in [20], one gets

$$V_q(x_{k+1}^*, E_{k+1}) \le \mu_3 V_p(x_k^*, E_k), \tag{53}$$

with

$$\begin{aligned}\mu_3 &= \max_{M\ni p\neq q\in M}\mu_{3pq}, \\ \mu_{3pq} &= \max\left\{\frac{2n\widetilde{P}_q h_{pq}^2 + 2\rho_q\alpha_{3,pq}^2}{\overline{P}_p}, \right. \\ &\quad \left. \cdot\frac{2n\widetilde{P}_q\widetilde{h}_{pq}^2}{\rho_p}\left(\frac{N-1}{N}\right)^2 + \frac{2\rho_q\beta_{3,pq}^2}{\rho_p}\right\}.\end{aligned} \tag{54}$$

4.2.2. An Attack Occurs at t_k. Let $r(t_k) = p$, $r(t_{k+1}) = q \neq p$, and $\sigma(t_k) = m$, it follows from (38) and (39) that

$$E_{k+1} \le \alpha_{4,mpq}\left\|x_k^*\right\| + \beta_{4,mpq}E_k, \tag{55}$$

where

$$\begin{aligned}\alpha_{4,mpq} &= \left(e^{\left\|\overline{A}_{mq}\right\|(h-t'')} + 1\right)\left\|e^{\overline{A}_{mq}t''}\right\|\left\|e^{\overline{A}_{mp}t'}\right\| \\ &\quad + e^{\left\|\overline{A}_{mq}\right\|h}e^{\left\|\overline{A}_{mp}\right\|h}, \\ \beta_{4,mpq} &= \alpha_{4,mpq}\frac{N-1}{N} + e^{\left\|\overline{A}_{mq}\right\|h}e^{\left\|\overline{A}_{mp}\right\|h}\frac{2N-1}{2N}, \\ \left\|x_{k+1}^*\right\| &\le \overline{h}_{mpq}\left(\left\|x_k^*\right\| + \frac{N-1}{N}E_k\right),\end{aligned} \tag{56}$$

with $\overline{h}_{mpq} = \|\overline{H}_{mpq}\|, \overline{H}_{mpq} = [I_{n*n}\,0_{n*n}]e^{\overline{A}_{mq}t''}e^{\overline{A}_{mp}t'}$.

Then, one gets the following:

$$\begin{aligned}&V_q(x_{k+1}^*, E_{k+1}) \\ &\quad = (x_{k+1}^*)^\top P_q(\tau_{k+1})x_{k+1}^* + \rho_q E_{k+1}^2 \\ &\quad \le n\widetilde{P}_q\left\|x_{k+1}^*\right\|^2 + \rho_q E_{k+1}^2 \\ &\quad \le n\widetilde{P}_q\overline{h}_{\mathrm{mpq}}^2\left(\left\|x_k^*\right\| + \frac{N-1}{N}E_k\right)^2 \\ &\qquad + \rho_q\left(\alpha_{4,\mathrm{mpq}}\left\|x_k^*\right\| + \beta_{4,\mathrm{mpq}}E_k\right)^2 \\ &\quad \le 2n\widetilde{P}_q\overline{h}_{\mathrm{mpq}}^2\left\|x_k^*\right\|^2 + 2n\widetilde{P}_q\overline{h}_{\mathrm{mpq}}^2\left(\frac{N-1}{N}\right)^2E_k^2 \\ &\qquad + 2\rho_q\alpha_{4,\mathrm{mpq}}^2\left\|x_k^*\right\|^2 + 2\rho_q\beta_{4,\mathrm{mpq}}^2E_k^2 \\ &\quad = \left(2n\widetilde{P}_q\overline{h}_{\mathrm{mpq}}^2 + 2\rho_q\alpha_{4,\mathrm{mpq}}^2\right)\left\|x_k^*\right\|^2 \\ &\qquad + \left(2n\widetilde{P}_q\overline{h}_{\mathrm{mpq}}^2\left(\frac{N-1}{N}\right)^2 + 2\rho_q\beta_{4,\mathrm{mpq}}^2\right)E_k^2 \\ &\quad \le \frac{2n\widetilde{P}_q\overline{h}_{\mathrm{mpq}}^2 + 2\rho_q\alpha_{4,\mathrm{mpq}}^2}{\overline{P}_p}(x_k^*)^\top P_p x_k^* \\ &\qquad + \left(\frac{2n\widetilde{P}_q\overline{h}_{\mathrm{mpq}}^2}{\rho_p}\left(\frac{N-1}{N}\right)^2 + \frac{2\rho_q\beta_{4,\mathrm{mpq}}^2}{\rho_p}\right)\rho_p E_k^2 \\ &\quad \le \mu_4 V_p(x_k^*, E_k),\end{aligned} \tag{57}$$

where

$$\begin{aligned}\mu_4 &= \max_{m\in M, M\ni p\neq q\in M}\mu_{4\mathrm{mpq}}, \\ \mu_{4\mathrm{mpq}} &= \max\left\{\frac{2n\widetilde{P}_q\overline{h}_{\mathrm{mpq}}^2 + 2\rho_q\alpha_{4,\mathrm{mpq}}^2}{\overline{P}_p}, \right. \\ &\quad \left. \cdot\frac{2n\widetilde{P}_q\overline{h}_{\mathrm{mpq}}^2}{\rho_p}\left(\frac{N-1}{N}\right)^2 + \frac{2\rho_q\beta_{4,\mathrm{mpq}}^2}{\rho_p}\right\}.\end{aligned} \tag{58}$$

5. Stability Analysis

To establish the stability of the closed-loop system (16), we first pursue the upper bound of Lyapunov function at t_k based on the analysis in Section 4. On this basis, the sufficient conditions ensuring exponential convergence in the mean sense of the closed-loop system are provided.

5.1. The Upper Bound of Lyapunov Function at t_k

Lemma 7. *Let $\widetilde{\mu} = \max\{\mu_2, \mu_3, \mu_4\} > 1$. If dwell time h and β defined in (7) meet*

$$\frac{1}{h} - \frac{1}{\beta} > \frac{\ln \widetilde{\mu}}{\ln \widetilde{\mu} - \ln \mu_1} > 0, \tag{59}$$

and $\overline{\pi}, \pi$ defined in Lemma 1 and α, ζ, T defined in Assumption 5 satisfy

$$\overline{\pi} \le \pi < \left(\frac{(1/\beta - 1/h)\ln(\mu_1/\widetilde{\mu}) - \ln \widetilde{\mu}}{1 + h/\beta} + \overline{\pi} \right) \frac{\mu_1}{\mu_3}, \tag{60a}$$

$$T > \max\left\{ \frac{\beta}{\beta - h}, \frac{1}{1 + (\pi\mu_3/\mu_1 - \overline{\pi})(1 + h/\beta) + \ln \widetilde{\mu}/\ln(\mu_1/\widetilde{\mu})h - h/\beta} \right\}, \tag{60b}$$

then the Lyapunov function follows the following property:

$$E\left\{ V_{\sigma(t_k)}(x_k^*, E_k) \right\} \le \overline{c}\theta^{\widetilde{\omega}k} \left(\max_{p \in M} \rho_p \right) E_0^2, \tag{61}$$

where

$$\begin{aligned} \overline{c} &= e^{(\pi(\mu_3/\mu_1) - \overline{\pi})(h\alpha - (h/\beta)t_0)} \left(\frac{\mu_1}{\widetilde{\mu}} \right)^{(t_0/T) - \zeta/h + (t_0/\beta)} \\ &\quad \times e^{(\pi(\mu_3/\mu_1) - \overline{\pi})(t_0/\beta - \alpha)h} \left(\frac{\mu_1}{\widetilde{\mu}} \right)^{(1 - (1/T)/h - 1/\beta)((t_0/\beta) - \alpha)h/1 + h/\beta)}, \\ \theta &= \widetilde{\mu} e^{((\mu_3/\mu_1)\pi - \overline{\pi})(1 + h/\beta)} \left(\frac{\mu_1}{\widetilde{\mu}} \right)^{(1 - (1/T)/h - 1/\beta)} < 1, \\ \widetilde{\omega} &= 1 + \frac{h}{\beta}. \end{aligned} \tag{62}$$

Proof. Assume that there are $\widetilde{m}$ time attacks that occur within the interval $[t_0, t_k)$. Denote $a_1, a_2, \ldots, a_{\widetilde{m}}$ and $a_1 + b_1, a_2 + b_2, \ldots, a_{\widetilde{m}} + b_{\widetilde{m}}$ as the beginning and ending instants of these attacks. Let $\widetilde{a}_i, \forall i \in \{1, 2, \ldots, \widetilde{m}\}$ be the first triggered instant after a_i.

Denote F_1 as the increasing/decreasing rate of the Lyapunov function during the interval $\cup_{i=1}^{\widetilde{m}} [\widetilde{a}_i, a_i + b_i)$ and F_2 as the one corresponding to $[t_0, t_k)/\cup_{i=1}^{\widetilde{m}} [\widetilde{a}_i, a_i + b_i)$. It is obvious that the increasing/decreasing rate of Lyapunov function from t_0 to t_k, denoted by F, meets $F = F_1 F_2$.

First, by recalling Lemma 1, (48), and (57), one has

$$\begin{aligned} F_1 &\le P(N_r(t) = 0)\mu_2^{k_1}\mu_4^0 + P(N_r(t) = 1)\mu_2^{k_1 - 1}\mu_4^1 \\ &\quad + \ldots + P(N_r(t) = k_1)\mu_2^0\mu_4^{k_1} \\ &\le e^{-\overline{\pi}\chi_1} \left(\frac{(\pi\chi_1)^0}{0!}\widetilde{\mu}^{k_1} + \frac{(\pi\chi_1)^1}{1!}\widetilde{\mu}^{k_1} + \ldots + \frac{(\pi\chi_1)^{k_1}}{k_1!}\widetilde{\mu}^{k_1} \right) \\ &\le e^{-\overline{\pi}\chi_1} \sum_{i=0}^{k_1} \frac{(\pi\chi_1)^i}{i!}\widetilde{\mu}^{k_1} \\ &\le e^{(\pi - \overline{\pi})\chi_1}\widetilde{\mu}^{k_1}, \end{aligned} \tag{63}$$

where k_1 represents the number of triggers within the interval $\cup_{i=1}^{\widetilde{m}}[\widetilde{a}_i, a_i+b_i)$ and χ_1 denotes the length of $\cup_{i=1}^{\widetilde{m}}[\widetilde{a}_i, a_i+b_i)$. Obviously, χ_1 meets $\chi_1 \le |\Xi(t_0,t_k)|$.

Second, let k_2 represent the number of triggers during $[t_0,t_k)/\cup_{i=1}^{\widetilde{m}}[\widetilde{a}_i, a_i+b_i)$ and χ_2 denote the length of $[t_0,t_k)/\cup_{i=1}^{\widetilde{m}}[\widetilde{a}_i, a_i+b_i)$. Then, we have

$$\chi_2 \le t_k - \left|\Xi(t_0,t_k)\right| + hn(t_0,t_k). \tag{64}$$

Similarly, one has

$$\begin{aligned}
F_2 &\le P(N_r(t)=0)\mu_1^{k_2}\mu_2^0 + P(N_r(t)=1)\mu_1^{k_2-1}\mu_3^1 \\
&\quad + \ldots + P(N_r(t)=k_2)\mu_1^0\mu_3^{k_2} \\
&\le e^{-\overline{\pi}\chi_2}\left(\frac{(\pi\chi_2)^0}{0!}\mu_1^{k_2}\mu_3^0 + \frac{(\pi\chi_2)^1}{1!}\mu_1^{k_2-1}\mu_3^1\right. \\
&\quad \left. + \ldots + \frac{(\pi\chi_2)^{k_2}}{k_2!}\mu_1^0\mu_3^{k_2}\right) \\
&\le e^{-\overline{\pi}\chi_2}\left(\frac{(\pi\chi_2)^0}{0!}\left(\frac{\mu_3}{\mu_1}\right)^0 + \frac{(\pi\chi_2)^1}{1!}\left(\frac{\mu_3}{\mu_1}\right)^1\right. \\
&\quad \left. + \ldots + \frac{(\pi\chi_2)^{k_2}}{k_2!}\left(\frac{\mu_3}{\mu_1}\right)^{k_2}\right)\mu_1^{k_2} \\
&\le e^{-\overline{\pi}\chi_2}\sum_{j=0}^{k_2}\frac{((\mu_3/\mu_1)\pi\chi_2)^j}{j!}\mu_1^{k_2} \\
&\le e^{(\mu_3/\mu_1\pi-\overline{\pi})\chi_2}\mu_1^{k_2}.
\end{aligned} \tag{65}$$

Combining the above two inequalities, one gets

$$F \le e^{(\pi-\overline{\pi})\chi_1}\widetilde{\mu}^{k_1}e^{(\mu_3/\mu_1\pi-\overline{\pi})\chi_2}\mu_1^{k_2}. \tag{66}$$

If $\pi \ge \overline{\pi}$ as shown in (60a), then $\pi-\overline{\pi}\ge 0$ and $\pi\mu_3/\mu_1-\overline{\pi}\ge 0$. Recalling $\chi_1 \le |\Xi(t_0,t_k)|$ and (64), one gets

$$\begin{aligned}
F &\le e^{(\pi-\overline{\pi})|\Xi(t_0,t_k)|}e^{(\mu_3/\mu_1\pi-\overline{\pi})(t_k-|\Xi(t_0,t_k)|+hn(t_0,t_k))}\widetilde{\mu}^{k_1}\mu_1^{k_2} \\
&= e^{(1-\mu_3/\mu_1)\pi|\Xi(t_0,t_k)|}e^{(\mu_3/\mu_1\pi-\overline{\pi})(t_k+hn(t_0,t_k))}\widetilde{\mu}^{k_1}\mu_1^{k_2} \\
&\le e^{(\mu_3/\mu_1\pi-\overline{\pi})(t_k+h(\alpha+t_k-t_0/\beta))}\widetilde{\mu}^{k_1}\mu_1^{k_2} \\
&= e^{(\mu_3/\mu_1\pi-\overline{\pi})\left(h\alpha-\frac{h}{\beta}t_0\right)}e^{(\mu_3/\mu_1\pi-\overline{\pi})(1+h/\beta)t_k}\widetilde{\mu}^{k_1}\mu_1^{k_2},
\end{aligned} \tag{67}$$

where the second inequality is based on $\mu_1 \le \mu_3$ and (7).

Considering that k_2 satisfies the following:

$$\begin{aligned}
k_2 &\ge \frac{t_k - \left|\Xi(t_0,t_k)\right|}{h} - n(t_0,t_k) \\
&\ge \frac{t_k-(\zeta+t_k-t_0/T)}{h} - \left(\alpha+\frac{t_k-t_0}{\beta}\right) \\
&= \left(\frac{t_0/T-\zeta}{h}+\frac{t_0}{\beta}\right)+\left(\frac{1-1/T}{h}-\frac{1}{\beta}\right)t_k,
\end{aligned} \tag{68}$$

we can obtain

$$\begin{aligned}
\widetilde{\mu}^{k_1}\mu_1^{k_2} &= \widetilde{\mu}^{k-k_2}\mu_1^{k_2} = \widetilde{\mu}^k\left(\frac{\mu_1}{\widetilde{\mu}}\right)^{k_2} \\
&\le \widetilde{\mu}^k\left(\frac{\mu_1}{\widetilde{\mu}}\right)^{(t_0/T)-\zeta/h+(t_0/\beta)}\left(\frac{\mu_1}{\widetilde{\mu}}\right)^{(1-(1/T)/h-1/\beta)t_k}.
\end{aligned} \tag{69}$$

Because $\mu_1 \le \widetilde{\mu}$, we combined (67) and (69), which yields

$$\begin{aligned}
F &\le e^{((\mu_3/\mu_1)\pi-\overline{\pi})(h\alpha-h/\beta t_0)}\left(\frac{\mu_1}{\widetilde{\mu}}\right)^{(t_0/T)-\zeta/h+(t_0/\beta)} \\
&\quad \times e^{((\mu_3/\mu_1)\pi-\overline{\pi})(1+(h/\beta))t_k}\widetilde{\mu}^k\left(\frac{\mu_1}{\widetilde{\mu}}\right)^{(1-1/T/h-1/\beta)t_k}.
\end{aligned} \tag{70}$$

On the one hand, by recalling $1/h > 1/\beta$ according to (59), there exists a large enough T such that

$$\frac{1-(1/T)}{h}-\frac{1}{\beta}>0. \tag{71}$$

On the other hand, based on the event-triggered scheme (3), it is easy to see that

$$t_k \ge (k-n(t_0,t_k))h \ge \left(k-\left(\alpha+\frac{t_k-t_0}{\beta}\right)\right)h, \tag{72}$$

i.e.,

$$t_k \ge \frac{kh}{1+h/\beta}+\frac{(t_0/\beta-\alpha)h}{1+h/\beta}. \tag{73}$$

If θ defined in (62) meets $\theta<1$, one has

$$e^{((\mu_3/\mu_1)\pi-\overline{\pi})(1+h/\beta)}\left(\frac{\mu_1}{\widetilde{\mu}}\right)^{(1-(1/T)/h-1/\beta)} < \theta < 1. \tag{74}$$

We summarized (70)–(74), which indicates that

$$\begin{aligned}
F &\le e^{(\pi\mu_3/\mu_1-\overline{\pi})(h\alpha-h/\beta t_0)}\left(\frac{\mu_1}{\widetilde{\mu}}\right)^{(t_0/T)-\zeta/h+(t_0/\beta)} \\
&\quad \cdot e^{(\pi(\mu_3/\mu_1)-\overline{\pi})((t_0/\beta)-\alpha)h} \\
&\quad \times\left(\frac{\mu_1}{\widetilde{\mu}}\right)^{(1-(1/T)/h-1/\beta)((t_0/\beta)-\alpha)h/1+h/\beta} \\
&\quad \times\left(\widetilde{\mu}e^{(\mu_3/\mu_1\pi-\overline{\pi})(1+h/\beta)}\left(\frac{\mu_1}{\widetilde{\mu}}\right)^{((1-1/T/h)-1/\beta)}\right)^{h/(1+h/\beta)k} \\
&= \overline{c}\theta^{\widetilde{\omega}k},
\end{aligned} \tag{75}$$

with $\overline{c}$, θ, and $\widetilde{\omega}$ defined in (62). By considering $x_0^* = 0$, one gets

$$E\left\{V_{\sigma(t_k)}\left(x_k^*, E_k\right)\right\} \le \overline{c}\theta^{\widetilde{\omega}k}\left(\max_{p\in M}\rho_p\right)E\left(t_0\right)^2. \tag{76}$$

To ensure $\theta < 1$, i.e.,

$$\left(\frac{\mu_3}{\mu_1}\pi - \overline{\pi}\right)\left(1 + \frac{h}{\beta}\right) + \ln\widetilde{\mu} + \left(\frac{1 - 1/T}{h} - \frac{1}{\beta}\right)\ln\frac{\mu_1}{\widetilde{\mu}} < 0, \tag{77}$$

T should satisfy

$$T > \frac{1}{1 + \left(\left(\left(\mu_3/\mu_1\right)\pi - \overline{\pi}\right)\left(1 + h/\beta\right) + \ln\widetilde{\mu}/\ln\mu_1/\widetilde{\mu}\right)h - h/\beta}. \tag{78}$$

Moreover, (60a) is used to guarantee that the denominator of lower bound of T is greater than 0 and (59) can ensure that the upper bound of π is a positive number.

From Lemma 7, we can get the following:

$$E\left\{\left\|x_k^*\right\|\right\} \le \sqrt{\frac{E\left(V\left(x_k^*, E_k\right)\right)}{\min\limits_{p\in M}\lambda\left(P_p\right)}} \le \frac{1}{\overline{c}2}\frac{\widetilde{\omega}}{\theta 2}k\sqrt{\frac{\max\limits_{p\in M}\rho_p}{\min\limits_{p\in M}\lambda\left(P_p\right)}}E\left(t_0\right), \tag{79}$$

and

$$E\left\{E_k\right\} \le \overline{c}^{1/2}\theta^{\left(\widetilde{\omega}/2\right)k}\sqrt{\frac{\max\limits_{p\in M}\rho_p}{\min\limits_{p\in M}\rho_p}}E\left(t_0\right). \tag{80}$$

5.2. Exponential Convergence in the Mean Sense of Closed-Loop System. This section will provide a structural proof for the following theorem. To achieve this, we modify the relevant calculations in Section 3.2.2, which is corresponding to the worst case, to derive simpler and more conservative boundaries.

Theorem 8. *Suppose that Assumptions 2, 4, and 5 hold. If the conditions in Lemma 7 are satisfied, there exists a coding and control strategy such that the closed-loop Markov jump system (16) achieves exponential convergence in the mean sense, i.e.,*

$$E\left(\left\|x\left(t\right)\right\|\right) \le \eta e^{-\omega t}g\left(\left\|x\left(0\right)\right\|\right), \forall t \ge 0, \tag{81}$$

holds for every initial condition x_0, where $\omega = \widetilde{\omega}/2h\log 1/\theta$, $\eta = \widetilde{\eta}\theta^{-\left(\widetilde{\omega}/2\right)}$, and

$$\widetilde{\eta} = \overline{c}^{1/2}\left(\widetilde{\alpha}\sqrt{\frac{\max\limits_{p\in M}\rho_p}{\min\limits_{p\in M}\lambda\left(P_p\right)}} + \widetilde{\beta}\sqrt{\frac{\max\limits_{p\in M}\rho_p}{\min\limits_{p\in M}\rho_p}}\right), \tag{82}$$

with $\widetilde{\alpha}$ and $\widetilde{\beta}$ defined in (90).

Proof. For all $t \in (t_k, t_k + \overline{t})$, by (25), one has

$$\left\|y\left(t\right) - \overline{y}\left(t - t_k\right)\right\| \le \max_{0\le s\le t-t_k}\left\|e^{\overline{A}_{mp}s}\right\|\frac{2N-1}{2N}E_k. \tag{83}$$

Because $\overline{y}\left(t - t_k\right) = e^{\overline{A}_{mp}\left(t-t_k\right)}\overline{y}\left(0\right)$ and $\widehat{x}\left(t_k\right) = \widetilde{c}_k$, it yields

$$\begin{aligned}&\left\|\overline{y}\left(t - t_k\right) - \overline{y}\left(0\right)\right\| \\ &\le \max_{0\le s\le t-t_k}\left\|e^{\overline{A}_{mp}s} - I\right\|\left\|\widetilde{c}_k\right\| \\ &\le \max_{0\le s\le t-t_k}\left\|e^{\overline{A}_{mp}s} - I\right\|\left(\left\|x_k^*\right\| + \frac{N-1}{N}E_k\right).\end{aligned} \tag{84}$$

By the triangle inequality, one gets

$$\begin{aligned}&\left\|y\left(t\right) - \overline{y}\left(0\right)\right\| \\ &\le \max_{0\le s\le t-t_k}\left\|e^{\overline{A}_{mp}s} - I\right\|\left(\left\|x_k^*\right\| + \frac{N-1}{N}E_k\right) \\ &\quad + \max_{0\le s\le t-t_k}\left\|e^{\overline{A}_{mp}s}\right\|\frac{2N-1}{2N}E_k \\ &:= \overline{D}_{k+1}\left(t - t_k\right).\end{aligned} \tag{85}$$

Specially, one has $\left\|y\left(t_k + \overline{t}\right) - \overline{y}\left(0\right)\right\| \le \overline{D}_{k+1}\left(\overline{t}\right)$.

Consider that the closed-loop dynamic is $\dot{y} = \overline{A}_{mq}y$ during the interval $[t_k + \overline{t}, t_{k+1})$. If we rewrite the second auxiliary system as

$$\dot{\widetilde{y}} = \overline{A}_{mq}\widetilde{y}, \widetilde{y}\left(0\right) = \overline{y}\left(0\right), \tag{86}$$

it is easy to see that

$$\left\|y\left(t\right) - \overline{y}\left(t - t_k - \overline{t}\right)\right\| \le \max_{0\le s\le t-t_k-\overline{t}}\left\|e^{\overline{A}_{mq}s}\right\|\overline{D}_{k+1}\left(\overline{t}\right), \tag{87}$$

holds for any $t \in [t_k + \overline{t}, t_{k+1})$. Because $\overline{y}\left(t - t_k - \overline{t}\right) = e^{\overline{A}_{mq}\left(t-t_k-\overline{t}\right)}\overline{y}\left(0\right)$, one gets

$$\begin{aligned}&\left\|\overline{y}\left(t - t_k - \overline{t}\right) - \overline{y}\left(0\right)\right\| \\ &\le \max_{0\le s\le t-t_k-\overline{t}}\left\|e^{\overline{A}_{mq}s} - I\right\|\left\|\overline{y}\left(0\right)\right\| \\ &\le \max_{0\le s\le t-t_k-\overline{t}}\left\|e^{\overline{A}_{mq}s} - I\right\|\left\|\widetilde{c}_k\right\| \\ &\le \max_{0\le s\le t-t_k-\overline{t}}\left\|e^{\overline{A}_{mq}s} - I\right\|\left(\left\|x_k^*\right\| + \frac{N-1}{N}E_k\right).\end{aligned} \tag{88}$$

Hence, we have

$$\begin{aligned}&\left\|y\left(t\right) - \overline{y}\left(0\right)\right\| \\ &\le \max_{0\le s\le h}\left\|e^{\overline{A}_{mq}s}\right\|\overline{D}_{k+1}\left(h\right) \\ &\quad + \max_{0\le s\le h}\left\|e^{\overline{A}_{mq}s} - I\right\|\left(\left\|x_k^*\right\| + \frac{N-1}{N}E_k\right) \\ &:= \overline{E}_{k+1}.\end{aligned} \tag{89}$$

Projecting onto the x-component, we deduce $\left\|x\left(t\right) - \widetilde{c}_k\right\| \le \overline{E}_{k+1}$, which implies that

$$\|x(t)\| \le \left\|\widetilde{c}_k\right\| + \left\|x(t) - \widetilde{c}_k\right\| \le \left\|x_k^*\right\| + \frac{N-1}{N}E_k + \overline{E}_{k+1} \coloneqq \widetilde{\alpha}\left\|x_k^*\right\| + \widetilde{\beta}E_k, \tag{90}$$

with $\widetilde{\alpha} = \max_{m,p,q\in M}\widetilde{\alpha}_{mpq}$, $\widetilde{\beta} = \max_{m,p,q\in M}\widetilde{\beta}_{mpq}$, and

$$\widetilde{\alpha}_{mpq} = 1 + \max_{0\le s\le h}\left\|e^{\overline{A}_{mq}s}\right\|\left\|e^{\overline{A}_{mp}s} - I\right\| + \max_{0\le s\le h}\left\|e^{\overline{A}_{mq}s} - I\right\|$$

$$\widetilde{\beta}_{mpq} = \widetilde{\alpha}_{mpq}\frac{N-1}{N} + \max_{0\le s\le h}\left\{\left\|e^{\overline{A}_{mq}s}\right\|\left\|e^{\overline{A}_{mp}s}\right\|\right\}\frac{2N-1}{2N}. \tag{91}$$

Combined (79) and (80) induces that

$$E(\|x(t)\|) \le \widetilde{\eta}\widetilde{\theta}^{\widetilde{\omega}k/2}E(t_0). \tag{92}$$

Based on the analysis in Section 3, one knows that the design of $E(t_0)$ relies on $\|x(0)\|$. Hence, there exists a function $g(\cdot)$ such that $E(t_0) = g(\|x(0)\|)$.

By defining $\omega = \widetilde{\omega}/2h\log 1/\theta$ and $\eta = \widetilde{\eta}\theta^{-\widetilde{\omega}/2}$, (92) implies that

$$E(\|x(t)\|) \le \eta e^{-\omega t}g(\|x(0)\|). \tag{93}$$

The proof is completed.

6. Simulation Example

The two-tank system borrowed from [24] is used to verify the effectiveness of the control strategy, which can be modeled as system (1) with $M = \{1, 2\}$ and

$$A_1 = A_2 = \begin{bmatrix} -1 & -2 \\ 1 & 0 \end{bmatrix}, \quad B_1 = \begin{bmatrix} -2 \\ 0 \end{bmatrix}, \quad B_2 = \begin{bmatrix} 0 \\ -1 \end{bmatrix}, \tag{94}$$

where the system states represent the deviations from the nominal reservoir levels. The flow between two tanks is proportional to the difference of the reservoir levels, and the flow control can be switched arbitrarily.

Let $x_0 = [3, 2]^\top$, $\overline{\delta} = 0.01$, $N = 5$, $E_0 = 0.1$, $\alpha = 1$, and $\zeta = 1$. Select $K_1 = [1\,0]$, $K_2 = [0\,2]$, and $h = 0.2$. To ensure (59) and ((60a) and (60b)), we set $\beta = 3$, $T = 3$, $\pi_{12} = 0.015$, and $\pi_{21} = 0.02$.

From Figure 2, it is obvious that $t_0 = 6$ can be selected as the initial triggered instant. The mean values of the system states are shown as the red lines in Figure 3, from which we can see that the closed-loop system is exponential convergence in the mean sense under the quantization control algorithm designed in this paper.

Moreover, E_k and $\|x(t_k) - x_k^*\|$ are displayed in Figure 4, which illustrates that the quantizer is unsaturated after t_0. In such figure, the blue vertical dotted lines indicate the switching instants, which are randomly generated according to $r(0) = 1$ and $\pi_{pq}, \forall p, q \in M$, and the red vertical dotted lines denote the beginning instants of deception attacks, which are assumed to be random variables following the independent and identically distributed variables with a probability of 23%. Obviously, both switches and attacks result in an increase in E_k and $\|x(t_k) - x_k^*\|$. It is worth mentioning that the growth rate of E_k is much greater than that of

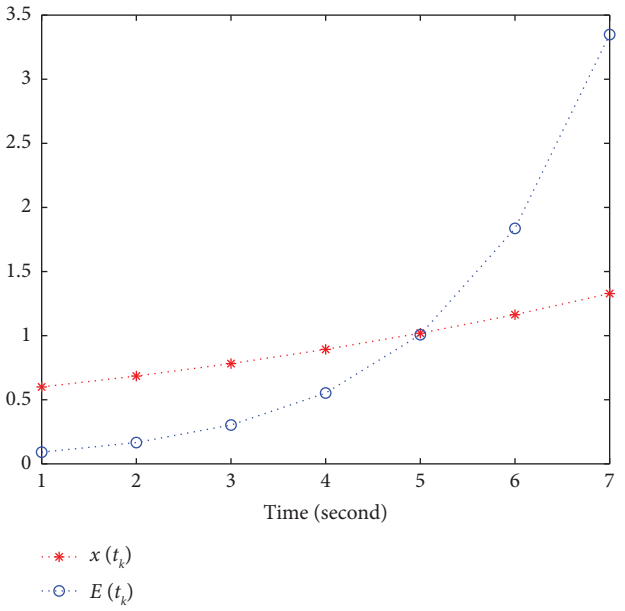

Figure 2: Selection of k_0.

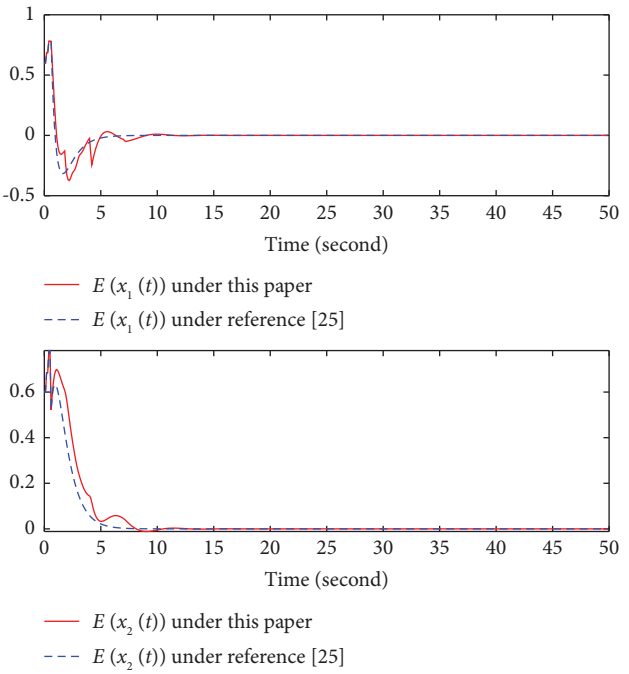

Figure 3: Comparison of the state trajectories of this paper and [25].

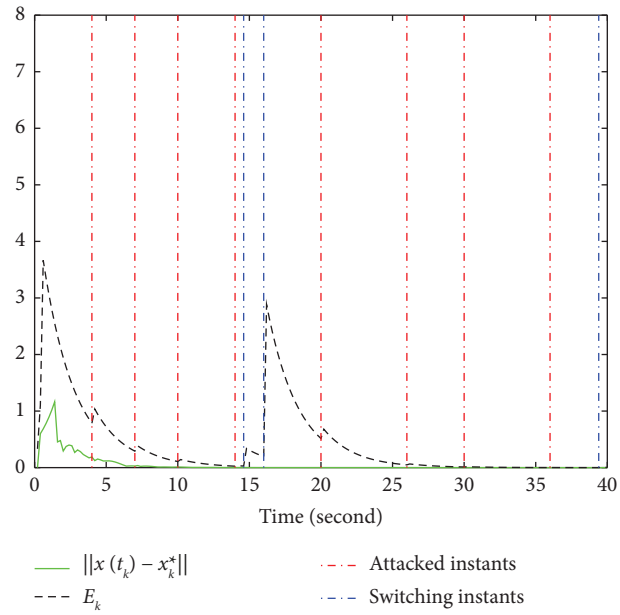

Figure 4: Unsaturation of quantizer.

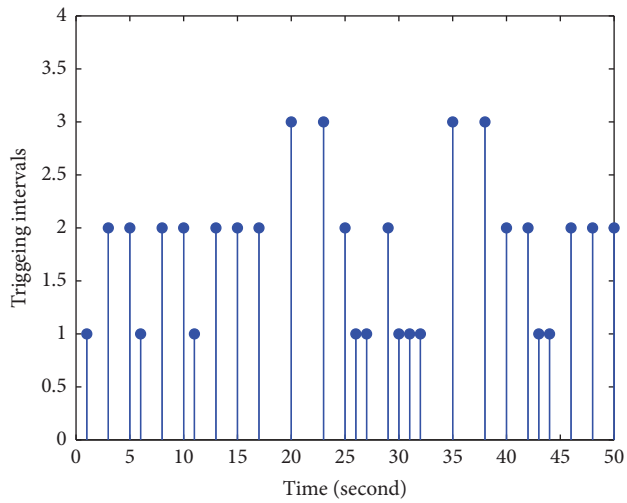

Figure 5: The triggering intervals in this paper.

$\|x(t_k) - x_k^*\|$. This is because E_k is designed from the worst case in order to ensure the unsaturation of the quantizer in all cases.

6.1. Comparison. As shown in Figure 3, by comparing the state trajectories of this paper and [25], where the triggered mechanism is designed without considering deception attacks, it can be seen that the convergence speed of this paper is slower than that of [25], and the oscillation amplitude of the state trajectories in this paper is greater than that of [25] under the influence of deception attacks. It means that the deception attacks inevitably reduce the system's performance. However, Figure 5 shows that the number of triggers within 50 seconds is 28 under the triggered mechanism proposed in this paper, but the one under the triggered

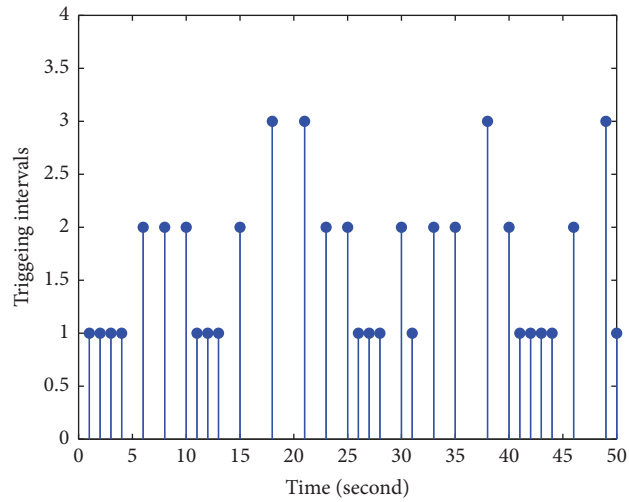

Figure 6: The triggering intervals in [25].

mechanism in [25] is 31 as shown in Figure 6. Hence, the algorithm proposed in this paper has certain advantages from the perspective of saving network resources.

7. Conclusions

The stabilization problem of the Markov jump systems with data quantization and deception attacks has been studied. By designing a suitable event-triggered scheme and quantization coding rules, the unsaturation of the quantizer at the triggered instants has been guaranteed. By analyzing the upper bound of the Lyapunov function, sufficient conditions ensuring the stability of the closed-loop system have been provided.

To simplify the analysis, this paper only considered a single channel. In fact, if the dual channel is executed, it means that the signal transmitted from the controller to the system has also suffered deception attacks, which brings challenges to the quantizer design. The quantized feedback control under bilateral network suffered deception attacks is one of our future research directions. Moreover, the triggered condition $t_{k+1} = t_k + h$ proposed in this paper is relatively conservative, which may result in more triggered times. How to remove such condition is another research direction in the future.

Data Availability

The data used to support the findings of this study are available from the corresponding author upon request.

Conflicts of Interest

The authors declare that they have no conflicts of interest.

Acknowledgments

The work was supported by the National Natural Science Foundation of China (61773154 and U1804163), the Training Plan of Young Backbone Teachers in Higher

Schools of Henan Province (2020GGJS085), and the Young Scholars Funding Program of Henan University of Technology (21420079).

References

[1] F. Vesentini, L. Di Persio, and R. Muradore, "A brownian-markov stochastic model for cart-like wheeled mobile robots," *European Journal of Control*, vol. 70, Article ID 100771, 2023.

[2] C.-H. Lin, K.-J. Wang, A. A. Tadesse, and B. H. Woldegiorgis, "Human-robot collaboration empowered by hidden semi-markov model for operator behaviour prediction in a smart assembly system," *Journal of Manufacturing Systems*, vol. 62, pp. 317–333, 2022.

[3] A. R. Somarin, P. Sharma, S. Tiwari, and S. Chen, "Stock reallocation policy for repairable service parts in case of supply disruptions due to extreme weather events," *International Journal of Production Economics*, vol. 256, Article ID 108743, 2023.

[4] X. Gao, F. Deng, H. Zhang, and P. Zeng, "Adaptive neural state estimation of Markov jump systems under scheduling protocols and probabilistic deception attacks," *IEEE Transactions on Cybernetics*, vol. 53, no. 3, pp. 1830–1842, 2023.

[5] Y. Zhang and Z.-G. Wu, "Asynchronous control of Markov jump systems under aperiodic DoS attacks," *IEEE Transactions on Circuits and Systems II: Express Briefs*, vol. 70, no. 2, pp. 685–689, 2023.

[6] J. Yu, M. Liu, and J. J. Rodriguez-Andina, "Zonotope-based asynchronous fault detection for Markov jump systems subject to deception attacks via dynamic event-triggered communication," *IEEE Open Journal of the Industrial Electronics Society*, vol. 3, pp. 304–317, 2022.

[7] Z. Ye, D. Zhang, J. Cheng, and Z.-G. Wu, "Event-triggering and quantized sliding mode control of UMV systems under DoS attack," *IEEE Transactions on Vehicular Technology*, vol. 71, no. 8, pp. 8199–8211, 2022.

[8] P. Chen, D. Zhang, L. Yu, and H. Yan, "Dynamic event-triggered output feedback control for load frequency control in power systems with multiple cyber attacks," *IEEE Transactions on Systems, Man, and Cybernetics: Systems*, vol. 52, no. 10, pp. 6246–6258, 2022.

[9] J. Lian and Y. Han, "Switching-like event-triggered control for networked Markovian jump systems under deception attack," *IEEE Transactions on Circuits and Systems II: Express Briefs*, vol. 68, no. 10, pp. 3271–3275, 2021.

[10] J. Cheng, L. Xie, D. Zhang, and H. Yan, "Novel event-triggered protocol to sliding mode control for singular semi-Markov jump systems," *Automatica*, vol. 151, Article ID 110906, 2023.

[11] Z. Zhang, Z. Chen, Z. Sheng, D. Li, and J. Wang, "Static output feedback secure synchronization control for Markov jump neural networks under hybrid cyber-attacks," *Applied Mathematics and Computation*, vol. 430, Article ID 127274, 2022.

[12] S.-T. Sun and X.-D. Li, "Quantized iterative learning control for nonlinear switched discrete-time systems with actuator saturation," in *Proceedings of the 2022 IEEE 11th Data Driven Control and Learning Systems Conference (DDCLS)*, pp. 1297–1302, Chengdu, China, August 2022.

[13] J. Li, G. Wei, D. Ding, and Y. Li, "Quantized control for networked switched systems with a more general switching rule," *IEEE Transactions on Systems, Man, and Cybernetics: Systems*, vol. 50, no. 5, pp. 1909–1917, 2020.

[14] S. Kamali, S. M. Tabatabaei, M. M. Arefi, and S. Yin, "Prescribed performance quantized tracking control for a class of delayed switched nonlinear systems with actuator hysteresis using a filter-connected switched hysteretic quantizer," *IEEE Transactions on Neural Networks and Learning Systems*, vol. 33, no. 1, pp. 61–74, 2022.

[15] W. Qi, M. Gao, C. K. Ahn, J. Cao, J. Cheng, and L. Zhang, "Quantized fuzzy finite-time control for nonlinear semi-markov switching systems," *IEEE Transactions on Circuits and Systems II: Express Briefs*, vol. 67, no. 11, pp. 2622–2626, 2020.

[16] T. Tan, J. Gao, J. Wang, Z. Zhao, and M. Ma, "Hybrid-driven mechanism based on uncertain network for Markov jump system with quantizations and delay," *Complexity*, vol. 2020, pp. 1–15, 2020.

[17] J. Cheng, Y. Wu, Z.-G. Wu, and H. Yan, "Nonstationary filtering for fuzzy Markov switching affine systems with quantization effects and deception attacks," *IEEE Transactions on Systems, Man, and Cybernetics: Systems*, vol. 52, no. 10, pp. 6545–6554, 2022.

[18] X. Zhou, Y. Tang, J. Cheng, J. Cao, C. Xue, and D. Yan, "Nonstationary quantized control for discrete-time Markov jump singularly perturbed systems against deception attacks," *Journal of the Franklin Institute*, vol. 358, no. 6, pp. 2915–2932, 2021.

[19] D. Chatterjee and D. Liberzon, "On stability of randomly switched nonlinear systems," *IEEE Transactions on Automatic Control*, vol. 52, no. 12, pp. 2390–2394, 2007.

[20] D. Liberzon, "Finite data-rate feedback stabilization of switched and hybrid linear systems," *Automatica*, vol. 50, no. 2, pp. 409–420, 2014.

[21] Z. Zhang, L. Zhang, F. Hao, and L. Wang, "Periodic event-triggered consensus with quantization," *IEEE Transactions on Circuits and Systems II: Express Briefs*, vol. 63, no. 4, pp. 406–410, 2016.

[22] F. Tang, H. Wang, X.-H. Chang, L. Zhang, and K. H. Alharbi, "Dynamic event-triggered control for discrete-time nonlinear Markov jump systems using policy iteration-based adaptive dynamic programming," *Nonlinear Analysis: Hybrid Systems*, vol. 49, Article ID 101338, 2023.

[23] Z. Zhao, J. Gao, and T. Zhang, "Dynamic output feedback control of discrete Markov jump systems based on event-triggered mechanism," *Journal of Control Science and Engineering*, vol. 2018, Article ID 4215147, 9 pages, 2018.

[24] M. Wakaiki and Y. Yamamoto, "Stability analysis of sampled-data switched systems with quantization," *Automatica*, vol. 69, pp. 157–168, 2016.

[25] Z. Ye, D. Zhang, Z.-G. Wu, and H. Yan, "A3C-based intelligent event-triggering control of networked nonlinear unmanned marine vehicles subject to hybrid attacks," *IEEE Transactions on Intelligent Transportation Systems*, vol. 23, no. 8, pp. 12921–12934, 2022.